AD-A158 029 REACTION INTERMEDIATES IN AROMATIC FUEL COMBUSTION(U) 1/1
CATHOLIC UNIV OF AMERICA WASHINGTON DC DEPT OF
CHEMISTRY W A SANDERS 17 JUL 84 N00014-83-K-0586

UNCLASSIFIED F/G 21/4 NL

END

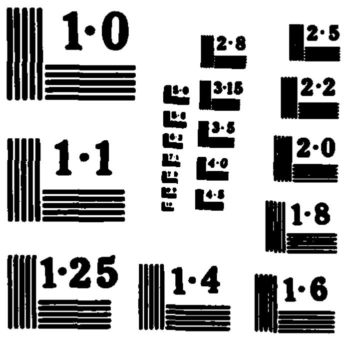

NATIONAL BUREAU OF STANDARDS
MICROCOPY RESOLUTION TEST CHART

AD-A158 029

(1)

Department of Chemistry

The Catholic University of America

Washington, DC 20064

REACTION INTERMEDIATES IN AROMATIC FUEL COMBUSTION

Final Report

Contract No.

N00014-83-K0586

Period

7-18-83 to 7-17-84

Principal Investigator: William A.Sanders

Scientific Program Officer: Dr. M. C. Lin
Naval Research Laboratory
Code 6180
4555 Overlook Ave., SW
Washington, DC 20375

ABSTRACT

The oxidation of benzene under fuel-lean conditions has been studied from 1600 to 2300 K in a shock tube using a stabilized CW CO laser to monitor CO production. The result of the kinetic modeling of the CO formation according to the global mechanism of Fujii and Asaba indicates that the rate of CO formation in the early stage of oxidation depends very sensitively on the rate-limiting unimolecular decomposition of benzene,

$$C_6H_6 \xrightarrow{1} C_6H_5 + H$$

The rate constant obtained for the initiation reaction using a scheme consisting of a set of 25 reactions is given by the following expression:

$$k_1 = 10^{15.70\pm0.52} \exp(-54{,}300 \pm 2200/T)\ \mathrm{sec}^{-1}.$$

for the pressure range of 1.9 - 2.7 atm. The result of an RRKM calculation for the reaction indicated that at temperatures above 2000 K, k_1 becomes slightly pressure-dependent. The extrapolation of the individual data with the RRKM theory led to

$$k_1^{\infty} = 10^{16.76\pm0.50} \exp(-58{,}400 \pm 2200/T)\ \mathrm{sec}^{-1}.$$

INTRODUCTION

There is considerable current interest in the kinetics and mechanism of benzene oxidation because of the increasing use of aromatics as fuel components. Partly due to the extremely complex mechanisms involved, to date there exist only a few high temperature kinetic studies (appropriate to combustion) on the oxidation of aromatics. Early shock tube studies on benzene oxidation[1-5] were concerned largely with ignition delays which could not be readily interpreted mechanistically.

Only in the more recent major works by Fujii and Asaba[6-10] using a shock tube and by Glassman and co-workers[11,12] using a high temperature adiabatic turbulent flow reactor, a clearer global picture of benzene oxidation began to emerge.

One common prominent feature found in the works of the aforementioned two groups, as well as in the low temperature study by Norrish and Taylor[13] is that CO is a major early product. However, the mechanism of CO formation remains largely speculative. To account for the observed CO formation, Fujii and Asaba[10] proposed the 'global' mechanism:

$$C_6H_6 + O_2 \longrightarrow 2CO + C_4H_4 + H .$$

Glassman and co-workers[11,12] proposed a detailed mechanism of CO formation involving the phenoxy radical. The high phenol concentration obtained in their work was proposed as evidence to this step. The detailed mechanism seems to be roughly consistent with Asaba's global scheme.[12]

In the present work, we used a shock tube to study the oxidation of benzene under extremely fuel-lean conditions under which the fast initial CO formation would be sensitive to the initiation step of phenyl radical formation. The real time CO concentration is measured by resonance absorption using a frequency-stabilized CW CO laser. Kinetic modeling of our CO profiles as well as its delay times, was made using a set of 25 reactions, based largely on Fujii and Asaba's global scheme to obtain information on the initiation reaction, $C_6H_6 \rightarrow C_6H_5 + H$, an important and poorly determined reaction in the benzene oxidation system.

EXPERIMENTAL

The details of the shock tube, the frequency-stabilized CW CO probe laser, CO absorption calibration, and other similar experimental procedures were given in previous publications.[14,15] In this work, only reflected shocks were used. All calculations for shocked gas properties such as temperature and pressure were made by using the NASA/LEWIS equilibrium program.[16] For all three reaction mixtures with C_6H_6:O_2:Ar ratios of 1:200:1799, 1:214:3011, and 1:218:6447, the $2 \rightarrow 1$ p(10) transition of the CO laser was used to measure the CO product concentration profiles by resonance absorption. CO threshold times were measured in other experiments using mixtures with ratios of 1:250:2070 and 1:263:2439. The laser output was continuously stabilized to line center by the use of a lock-in stabilizer.[14,15,17] Since substantial concentrations of O_2 were used in the C_6H_6-O_2-Ar reaction mixtures, the effective room temperature collision half-width γ° for CO, which accounts for pressure broadening in the CO absorption linewidth, was taken to be:[18]

$$\gamma^{\circ} = \gamma^{\circ}_{CO-O_2} X_{O_2} + \gamma^{\circ}_{CO-Ar} X_{Ar} \quad (1)$$

where X_{O_2} and X_{Ar} are the molefractions of O_2 and Ar. $\gamma^{\circ}_{CO-O_2}$ = 0.0452 cm^{-1} atm^{-1} (Ref. 15) and γ°_{CO-Ar} = 0.0522 cm^{-1} atm^{-1} (Ref. 14) are the room temperature collision half-widths of CO with O_2 and Ar as collision partners, respectively. The conversion of the absorption measurements to absolute CO concentrations was achieved by the use of the calibrated gain equation in Ref. 14.

We have also examined the possibility of UV emission by electronically excited species such as $C_6H_6^*$ and $C_6H_5OH^*$ in the 250 nm region. Emission measurements were made by using a 1P28 photomultiplier with a 254 nm band filter which has a FWHM band width of 10 nm. That emission was indeed present will be shown and discussed below.

Certified A.C.S. benzene from Fisher Scientific was purified by first partially crystalizing it at about 279K in a previously evacuated cold finger. Then the liquid-solid mixture was pumped for several minutes to preferentially remove any of the more volatile impurities. The mixture was then completely thawed out, and the same procedure was repeated two more times. GC analysis of the benzene samples before and after purification showed a large reduction in the impurities and the purified sample showed an impurity level of only < 0.002%.

KINETIC MODELING AND RESULTS

Reflected shock experiments have been carried out in the temperature range from 1600 to 2313 K and pressure range from 1.9 to 2.7 atm. for five $C_6H_6/O_2/Ar$ mixtures with C_6H_6 molefraction: 0.015%, 0.031%, 0.037%, 0.043%, and 0.050% and the O_2/C_6H_6 ratio of 200, 214, 250, 263 and 218.

Typical CO absorption and 254 nm emission traces are shown in Fig. 1(a) and 1(b) respectively. It should be mentioned here that the delay time in the emission correlates closely to that in the CO absorption trace. Typical CO concentration time profies at 2275, 2076, and 1743 K are shown by the circles in Figs. 2(a), 2(b) and 2(c) respectively. A conspicuous feature of these profiles is the relatively long induction (or appearance) times, followed by rapid production of CO with maxima approaching the total carbon limit. This suggests a high activation energy initiation step, followed by fast radical reactions which rapidly convert the hydrocarbon species (i.e., C_6H_6, C_6H_5, C_2H_2, CH_2, etc.) to CO and subsequently to CO_2.

To interpret our CO production results, we carried out kinetic modeling using a set of 25 reactions as shown in Table I, based largely on the global mechanism of Fujii and Asaba, established according to their data obtained from 300 nm UV absorption, 5 μm CO emission as well as end product analysis (in single-pulsed shock experiments).[10] We have neglected the $C_6H_6 + O_2 \rightarrow C_6H_5 + HO_2$ reaction in our present scheme because according to the rate constant estimated from transition-state-theory calculations by Lin and Tevault[31], its total reaction rate, even at out O_2 concentrations, at 1600 K (the lower temperature limit in our experiment), is 10^4 times less than that of benzene decomposition (Reaction (1)). The contribution of this biomolecular initiation reaction was found to be less than 5% of the total initiation rate in the worst case employed in this work when Fujii and Asaba's unusually large rate constant

$$(k = 6.3 \times 10^{13}\ e^{-30,000/T},\ \text{cc/mole·sec})^{10}$$

was used. Their value, however, was established on the basis of the low C-H bond dissociation energy in benzene, 427 kJ/mole (which is to be compared with the presently accepted value, 464 ± 8 kJ/mole as will be discussed later).

The reactions $C_6H_5 \rightarrow C_2H_2 + C_4H_3$ and $C_6H_6 + C_6H_5 \rightarrow$ biphenyl + H were also excluded in our modeling in view of our extremely O_2 - rich conditions. The inclusion of these reactions was found to have little effect on CO product profiles according to the result of out test modeling. The following acetylene-related reactions were added to the scheme: $C_2H_2 + O \rightarrow HC_2O + H$, $C_2H_2 + O \rightarrow CH_2 + CO$, $CH_2 + O_2 \rightarrow HCO + OH$, and $HC_2O + O_2 \rightarrow 2CO + OH$. We have adopted Fujii and Asaba's fast "global" reaction for CO production from the $C_6H_5 + O_2 \rightarrow 2CO + C_4H_4 + H$ reaction, as this reaction was essential for the successful modeling of our CO profiles, as revealed by our sensitivity analysis to be discussed later. In the modified mechanism, the only initiation step is Reaction (1), the unimolecular decomposition of benzene. In modeling our CO profiles, it was found that good fits could be obtained by varying only k_1. Typical modeling results are shown by the solid curves in Fig. 2.

The quality of our modeling of the CO formation profiles is also indicated by the close agreement of the experimental and modeled threshold (τ_o) as well as the time required to reach half of the maximum CO yield ($\tau_{\frac{1}{2}}$), as shown in Fig. 3.

The extracted k_1 values for benzene decomposition obtained from modeling the CO profiles are presented in the Arrhenius plot in Fig. 4. Also plotted in the figure are k_1 values obtained from modeling CO threshold time τ_o from eight experiments in which only threshold time information was available. A least squares fit of these points yields the following expression:

$$k_1 = 10^{15.70 \pm 0.52} \exp(-54300 \pm 2200/T) \text{ sec}^{-1}.$$

Also included in Fig.4 are Fujii and Asaba's data,[10] covering temperatures from 1200 to 1900 K. The agreement between the two sets of data is good considering the drastically different conditions employed in these experiments. In order to test the validity of our k_1 obtained from the modeling, a crude sensitivity analysis has been carried out at 2076 K (run corresponding to Fig. 2(b)) for 15 reactions in Table I which include the key reactions involving carbon-containing species. Each of the rate constants was varied by a factor of two up or down and the percent change in CO concentration at $\tau_{\frac{1}{2}}$ time was noted. The sensitivity test results are given in the right-hand column in Table I.

We have carried out an RRKM calculation to check the effect of pressure on k_1 over the whole range of temperature (1600 - 2300 K) and pressure (1.9 - 2.7 atm) studied based on Troe's weak collision assumption.[32] It was found that at temperatures above 2000 K, k_1 becomes slightly pressure-dependent. The extrapolation of all data points using an average energy transfer step-size of 1.5 kcal/mole for the oxygen-rich mixtures employed led to the value of $k_1^{\infty} = 10^{16.76 \pm 0.50} \exp(-58,400 \pm 2200/T)\ sec^{-1}$.

DISCUSSION

Although the mechanism of Fujii and Asaba[8-10] established under fuel rich and lower temperature conditions was globally crude, it was found to be sufficient to account for our CO production profiles measured under much different, fuel lean and higher temperature, conditions. The fitted rate constant for the rate-limiting initiation reaction

$$C_6H_6 \rightarrow C_6H_5 + H$$

is reasonable in terms of the values of both A-factor (6×10^{16} sec^{-1}) and activation energy (485 ± 18 kJ/mole). The latter gives rise to the energy barrier at OK, E_o = 463 kJ/mole, which is in close agreement with the recently accepted bond dissociation energy, $D(C_6H_5 - H)$ = 464 ± 8 kJ/mole.[33]

This global mechanism can account not only for the observed CO production threshold and half-maximum times, but also qualitatively for the observed profiles of the UV emission at 254 nm as shown in Fig. 5. This emission derives most likely from the electronically excited phenol at the S_1 state, which lies approximately 443 kJ/mole above the ground (S_0) state.[34,35] Since no such emission was detected in the shock heating of C_6H_5OH or C_6H_6 in Ar under similar conditions, the following chemical pumping processes are energetically most likely candidates for the production of the excited C_6H_5OH:

$$O + C_6H_6 \rightarrow C_6H_5OH^{*\dagger}, \ \Delta H^0 = -429 \text{ kJ/mole}$$

$$C_6H_5 + OH \rightarrow C_6H_5OH^{*\dagger}, \ \Delta H^0 = -464 \text{ kJ/mole}$$

where "*" and "†" represent electronic and vibrational excitation respectively. The energies available for the electronic excitation at 2000 K are approximately $E_{av} = -\Delta H^0 + 3RT =$ 480 kJ/mole in the $O + C_6H_6$ reaction and $E_{av} = -\Delta H^0 + 4\ RT$ = 530 kJ/mole in the $C_6H_5 + OH$ reaction. Although both reactions are not included in the global scheme, the profiles calculated from $I \propto [O][C_6H_6]$ and $[C_6H_5][OH]$ are in qualitative agreement with the observed UV emission profiles as shown in Fig. 5. This finding is another indication that the global scheme of Fujii and Asaba is adequate for the description of the <u>overall</u> oxidation kinetics.

The apparent usefulness of the global scheme in describing our present findings lies perhaps in the correctness of the value of the rate constant assigned by Fujii and Asaba for the overall chain propagation step:

$$C_6H_5 + O_2 \rightarrow 2CO + C_4H_4 + H.$$

This abridged step, as has been discussed by Glassman and coworkers,[12] could represent the following plausible sequence of events: $C_6H_5 + O_2 \rightarrow O + C_6H_5O \rightarrow (O + C_5H_5) + CO \rightarrow CO + C_5H_5O \rightarrow 2CO + C_4H_4 + H$. On the other hand, it is also likely that the elementary reaction,

$C_6H_5 + O_2 \rightarrow C_6H_5OO\cdot \rightarrow$ 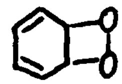 $+H$

$\rightarrow 2CO + C_4H_4 + H$

may occur at combustion temperatures.

At present we cannot differentiate one electronic excitation process from the other. We believe, however, that the $O + C_6H_6$ reaction is the key process responsible for the UV chemiluminescence because a direct test for the reaction using N_2O as the O atom source revealed an immediate appearance of the 254 nm emission with no delay at 1700 K, at which the dissociation of C_6H_6 is slow. Additionally, the concentration of C_6H_5 may be in reality not as high as that predicted by the global scheme employed here. It is quite possible that the key chain-carrying reactions involving the reaction C_6H_6 with O[36] and OH[37] occur mainly by the replacement processes via addition, rather than by abstraction yielding C_6H_5, even at these high temperatures: viz.,

$$O + C_6H_6 \rightarrow C_6H_5OH^{*\dagger} \rightarrow C_6H_5O + H$$

$$\Delta H^0 = -66.5 \text{ kJ/mole}$$

$$OH + C_6H_6 \rightarrow C_6H_6OH^{\dagger} \rightarrow C_6H_5OH + H$$

$$\Delta H^0 = -0.8 \text{ kJ/mole.}$$

The occurrence of these reactions can account for the production of large amounts of C_6H_5OH and its decomposition products, CO, C_5H_6, C_4H_6, etc., as recently reported by Glassman and coworkers.[12]

Obviously, the global scheme of Fujii and Asaba is mechanistically too crude to account for the production of C_6 and C_5 intermediates. Any realistic mechanism proposed for C_6H_6 oxdidation therefore should include these key intermediates and account for their formation and disappearance. To achieve this goal, evidently, much more kinetic data are needed, particularly with regard to various key elementary reactions involving $C_6(C_6H_6, C_6H_5OH, C_6H_5)$, $C_5(C_5H_5, C_5H_6)$, $C_4(C_4H_4, C_4H_6)$ and C_3H_x with O, H and OH over a broad range of temperature and pressure. Almost all of these reactions are expected to occur via stable adducts which may readily branch into diverse products at high temperatures. Further study is underway at this laboratory for the elucidation of the mechanisms of these processes.

CONCLUDING REMARKS

In this work we have studied the formation of CO in the oxidation of benzene in shock waves under fuel lean conditions employing the CO laser resonance absorption technique. Kinetic modeling of CO production profiles based largely on Fujii and Asaba's global mechanism gave rise to the extrapolated high-pressure rate constant for the key initiation reaction,

$$C_6H_6 \rightarrow C_6H_5 + H:$$

$$k_1^{\infty} = 6 \times 10^{16}\ e^{-58,400/T}\ \text{sec}^{-1}.$$

These Arrhenius parameters appear to be reasonable in comparison with the extrapolated values for toluene decomposition under high pressure conditions.[38]

Although the reliability of k_1 thus derived depends on the validity of the mechanism assumed, the "reasonableness" of its parameters and its ability to simulate CO production profiles over the broad range of conditions employed (as shown in Figures 2 and 3) seem reassuring. The ultimate checking of this rate constant would have to rely on the direct diagnostics of either H or C_6H_5 formed in the reaction.

References

1. Kogarko, S. M. and Borisov, A. A., Bull. Acad. Sci USSR 8, 1255 (1960).
2. Serbinov, A. I., Troshin, Ya. K. and Shchelkin, K. I., Proc. Acad. Sci USSR, Phys. Chem. Sec. 145, 602 (1962).
3. Orr, C. R., Ninth Symposium (International) on Combustion, p. 1034, Academic Press (1963).
4. Miyama, H., J. Chem. Phys. 52, 3850 (1970).
5. Miyama, H. J. Phys. Chem. 75, 1501 (1971).
6. Asaba, T. and Fujii, N., Thirteenth Symposium (International) on Combustion, p.155, The Combustion Institute (1971).
7. Asaba, T., and Fujii, N., Shock Tube Research, No. 46, Chapman and Hall, London (1971).
8. Fujii, N. and Asaba, T., Fourteenth Symposium (International) on Combustion, p.433, The Combustion Institute (1973).
9. Fujii, N. and Asaba, T., Acta Astronautica 1, 417 (1974).
10. Fujii, N. and Asaba, T., J. Faculty of Engineering, Univ. of Tokyo (B), XXXIV, No. 1, 189 (1977).
11. Santoro, R. J. and Glassman, I., Combustion Science and Technology 19, 161 (1979).
12. Venkat, C., Brezinsky, K. and Glassman, I., Nineteenth Symposium (International) on Combustion, p.143, The Combustion Institute (1982).
13. Norrish, R. G. W. and Taylor, G. W., Proc. Roy. Soc. A234, 160 (1956).

14. Hsu, D. S. Y., Shaub, W. M., Blackburn, M., and Lin, M. C., Nineteenth Symposium (International) on Combustion, p.89, The Combustion Institute (1982).

15. Hsu, D. S. Y., Shaub, W. M., Creamer, T., Gutman, D., and Lin, M. C., Ber. Bunsenges. Phys. Chem. 87, 909 (1983).

16. Gordon, S. and McBride, B. J., NASA SP-273, NASA, Washington, D. C. (1976).

17. Lin, M. C. and Shortridge, R. G., Chem. Phys. Lett. 29, 42 (1974).

18. Varghese, P. L. and Hanson, R. K., J. Quant. Spectrosc. Radiat. Transf 26, 339 (1981).

19. Löhr, R. and Roth, P., Ber. Bunsenges. Phys. Chem. 85, 153 (1981).

20. Browne, W. B., Twelfth Symposium (International) on Combustion, p.1035, The Combustion Institute (1969).

21. Vandooren, J., Sixteenth Symposium (International) on Combustion, p.1133, The Combustion Institute (1977).

22. Jones, I. T., Fourteenth Symposium (International) on Combustion, p.277, The Combustion Institute (1973).

23. Westbrook, C. K., J. Phys. Chem. 81, 1542 (1977).

24. Schecker, H. G. and Jost W., Ber. Bunsegos. Phys. Chem. 73, 521 (1969).

25. Baulch, D. L., Drysdale, D. D., Duxbury, J., and Grant, S., 'Evaluated Kinetic Data for High Temperature Reactions,' Vol. 3 (1976).

26. Hardy, J. E., Gardiner, W. C., Int. J. Chem. Kinet. 10, 503 (1979).

27. Schott, G. L., Getzinger, R. W. and Seitz, W. A., Int. J. Chem. Kinet. 6, 921 (1974).

28. Dixon-Lewis, 'Comp. Chem. Kinet.' 17, p.1 (1977).

29. Schott, G. L., Combust. Flame 21, 457 (1973).

30. Baulch, D. L., Drysdale, D. D., Horne, D. G., and Lloyd, A. C., 'Evaluated Kinetic Data for High Temperature Reactions,' Vol. 1 (1972).

31. Lin, M. C. and Tevault, D. E., Combust. Flame 42, 139 (1981).

32. Troe, J., J. Phys. Chem., 83, 114 (1979).

33. Golden. D. M., Ann. Rev. Phys. Chem. 33, 493 (1982).

34. Teuber, H. J. and Schmidtke, W., Chem. Ber. 93, 1257 (1960).

35. Zimmerman, H. and Joop, N., Z. Electrochem. 65, 61 (1961).

36. Sibener, S. J., Buss, R. J., Casavecchia, P., Hirooka, T., and Lee, Y. T., J. Chem. Phys. 72, 4341 (1980).

37. Tully, F. P., Ravishankara, A. R., Thompson, R. L., Nicovich, J. M., Shah, R. C., Kreutter, N. M., and Wine, P. H., J. Phys. Chem. 85, 2262 (1981).

38. Astholz, D. C., Durant, J. and Troe, J., 18th Intern. Symp. on Combustion, Combustion Institute, Pittsburgh, 1981, p.885.

Table I

Reactions and Rate Constants[a] Used in the Modeling of CO

Formed in the $C_6H_6 + O_2$ System

Reaction	A	B	Ea/R	Ref.	Sensitivity %[CO] Change 2k	k/2
(1) $C_6H_6 \rightarrow C_6H_5 + H$	to	be	fitted		+37	-34
(2) $C_6H_5 + O_2 \rightarrow 2CO + H + C_4H_4$	1.0×10^{12}	0	1010	10	+19	-27
(3) $C_6H_6 + O \rightarrow C_6H_5 + OH$	3.2×10^{14}	0	3020	10	+8	-10
(4) $C_6H_6 + OH \rightarrow C_6H_5 + H_2O$	1.0×10^{14}	0	3020	10	+18	-14
(5) $C_6H_6 + H \rightarrow C_6H_5 + H_2$	7.9×10^{13}	0	5030	10	0	0
(6) $C_4H_4 \rightarrow 2C_2H_2$	3.2×10^{14}	0	17610	10	0	0
(7) $C_2H_2 + O \rightarrow HC_2O + H$	4.3×10^{14}	0	6140	19	+10	-6
(8) $C_2H_2 + O \rightarrow CH_2 + CO$	1.2×10^{14}	0	3320	19	+6	-5
(9) $C_2H_2 + OH \rightarrow C_2H + H_2O$	6.0×10^{12}	0	3520	20,21	+2	-1
(10) $C_2H_2 + H \rightarrow C_2H + H_2$	2.0×10^{14}	0	9560	20	0	0
(11) $HC_2O + O_2 \rightarrow 2CO + OH$	1.5×10^{12}	0	1260	22	2	-3
(12) $CH_2 + O_2 \rightarrow HCO + OH$	1.0×10^{14}	0	1860	23	0	0
(13) $C_2H + O_2 \rightarrow HCO + CO$	1.0×10^{13}	0	3520	20	0	0
(14) $HCO + M \rightarrow CO + H + M$	1.6×10^{14}	0	7400	24	-	-

Table I (continued)

Reactions and Rate Constants[a] Used in the Modeling of CO

Formed in the $C_6H_6 + O_2$ System

Reaction	A	B	Ea/R	Ref.	Sensitivity %[CO] Change 2k	k/2
(15) $CO + OH \rightarrow CO_2 + H$	$\log_{10}k = 10.83 + 3.94 \times 10^{-4}T$			25	0	0
(16) $CO + O_2 \rightarrow CO_2 + O$	2.5×10^{12}	0	24000	25	-	-
(17) $CO + O + M \rightarrow CO_2 + M$	3.2×10^{13}	0	-2110	26	-	-
(18) $CO_2 + H \rightarrow CO + OH$	1.5×10^{14}	0	13390	25	-	-
(19) $H_2 + O \rightarrow H + OH$	1.5×10^{14}	0	6890	27	-	-
(20) $H_2 + OH \rightarrow H + H_2O$	1.2×10^{9}	1.3	1820	28	-	-
(21) $H + O_2 \rightarrow OH + O$	1.2×10^{17}	-0.91	8350	29	-	-
(22) $H + O_2 + M \rightarrow HO_2 + M$	1.6×10^{15}	0	-500	30	-	-
(23) $H + OH + M \rightarrow H_2O + M$	8.4×10^{21}	-2.0	0	30	-	-
(24) $H + H + M \rightarrow H_2 + M$	6.3×10^{17}	-1.0	0	30	-	-
(25) $O + O + M \rightarrow O_2 + M$	1.9×10^{13}	0	-900	25	-	-

a. In cc, mole, s units, in form $k = AT^{B}\exp(-E_a/RT)$

Figure Captions

Fig. 1. - Typical CO absorption trace (a) and 254 nm emission trace (b) at 1792 K and 2.37 atm for a 1:250:2070 ($C_6H_6:O_2:Ar$) mixture. The bottom trace in each panel is the pressure trace.

Fig. 2. - Typical CO concentration-time profiles for a 1:200:1799 ($C_6H_6:O_2:Ar$) mixture at (a) 2275 K, 2.00 atm., (b) 2076 K, 2.10 atm., and (c) 1743 K, 2.4 atm. Circles are experimental data and solid curves are modeled fits using the scheme in Table I. The total carbon content in each experiment is indicated by the line denoted by C_{tot}.

Fig. 3. - Normalized CO threshold (τ_0, circles) and half maximum ($\tau_{1/2}$, triangles) times for a 1:200:1799 ($C_6H_6:O_2:Ar$) mixture. Open symbols are experimental points and filled symbols are results from modeling. See text.

Fig. 4. - Arrhenius plot of k_1 extracted from modeling of CO profiles for $C_6H_6:O_2:Ar$ mixtures (○ - 1:200:1799, □ - 1:214:3011, △ - 1:218:6447) and by modeling of CO threshold times for mixtures (● - 1:250:2070, ▲ - 1:263:2439). Result of a least squares analysis is shown by the solid line. The dashed curve is Fujii and Asaba's results valid from 1200 to 1900 K. k_1^{∞} given by the dotted line is the extrapolated high-pressure rate constant (see text).

Figure Captions (continued)

Fig. 5. - 254 nm emission profiles at 2207, 2057, and 1738 K for a 1:250:2070 (C_6H_6:O_2:Ar) mixture. Circles are experimental data. Solid and dashed profiles are calculated respectively from I ∝ $[C_6H_6][O]$ and $[C_6H_5]$ [OH], where the concentrations as a functions of time were obtained from kinetic modeling. See text.

(a)

(b)

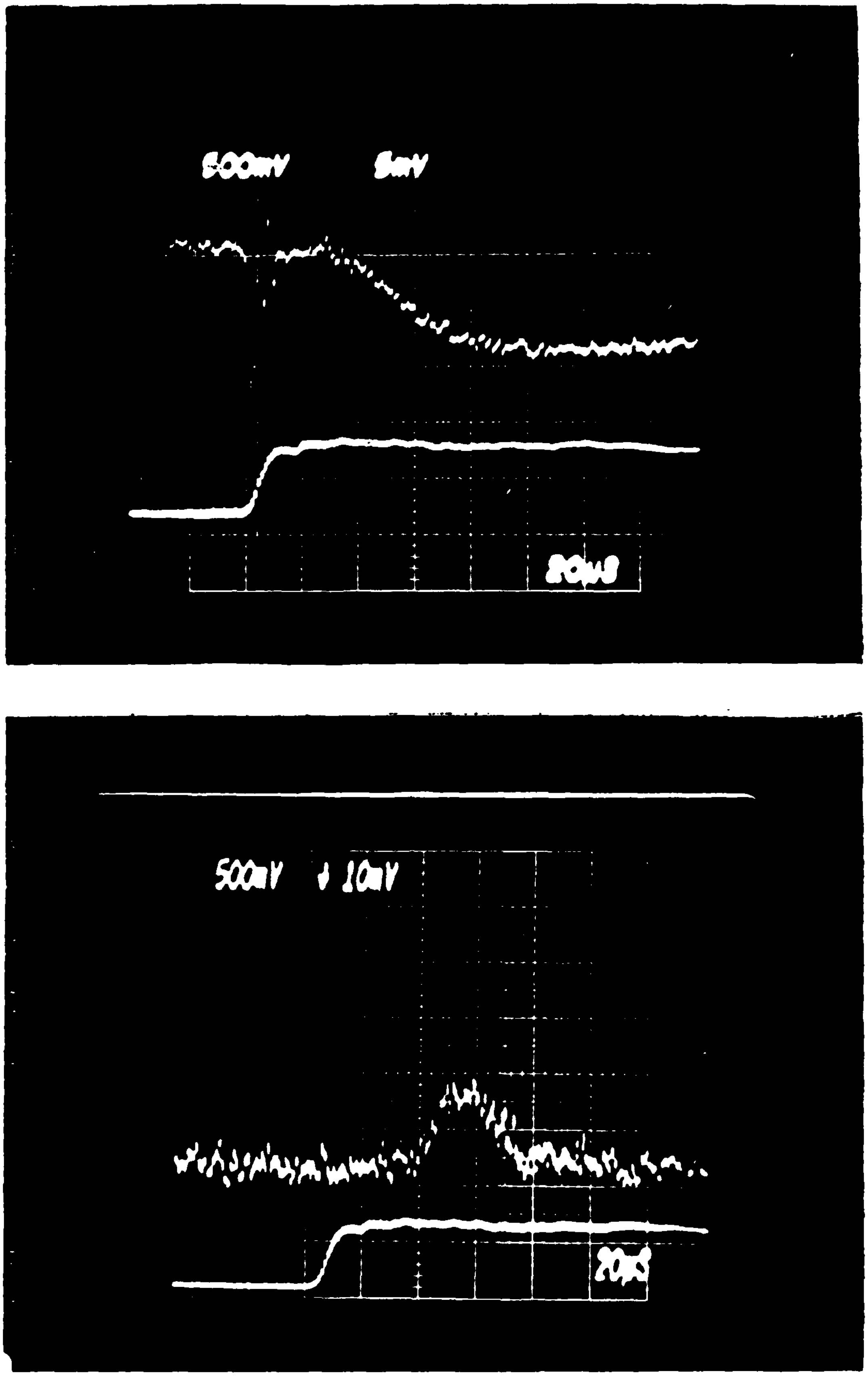

Fig 1.

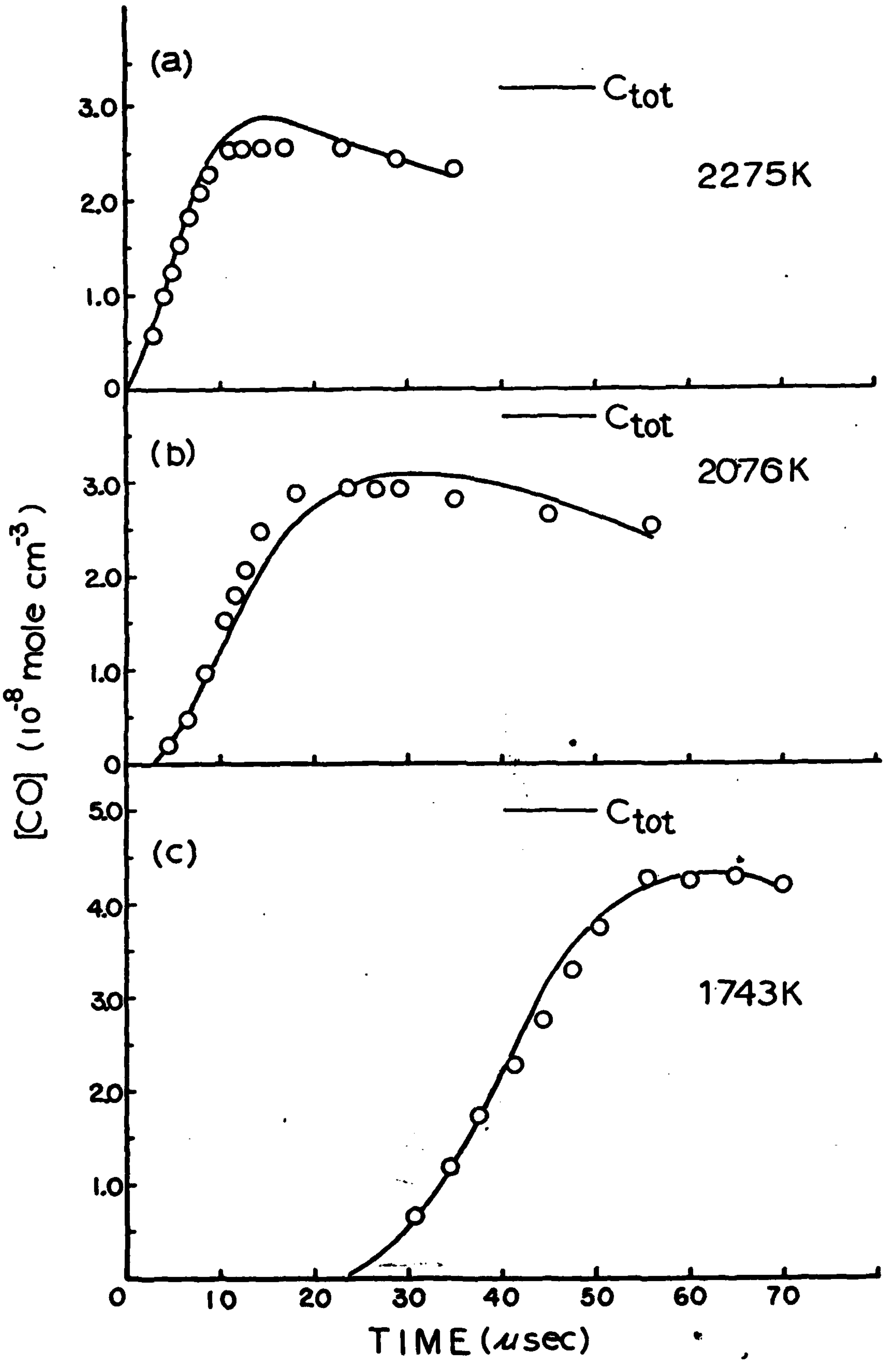
(a)
Ctot
2275K
(b)
Ctot
2076K
(c)
Ctot
1743K
[CO] (10^{-8} mole cm^{-3})
TIME (μsec)
0
10
20
30
40
50
60
70
3.0
2.0
1.0
5.0
4.0

Fig. 2.

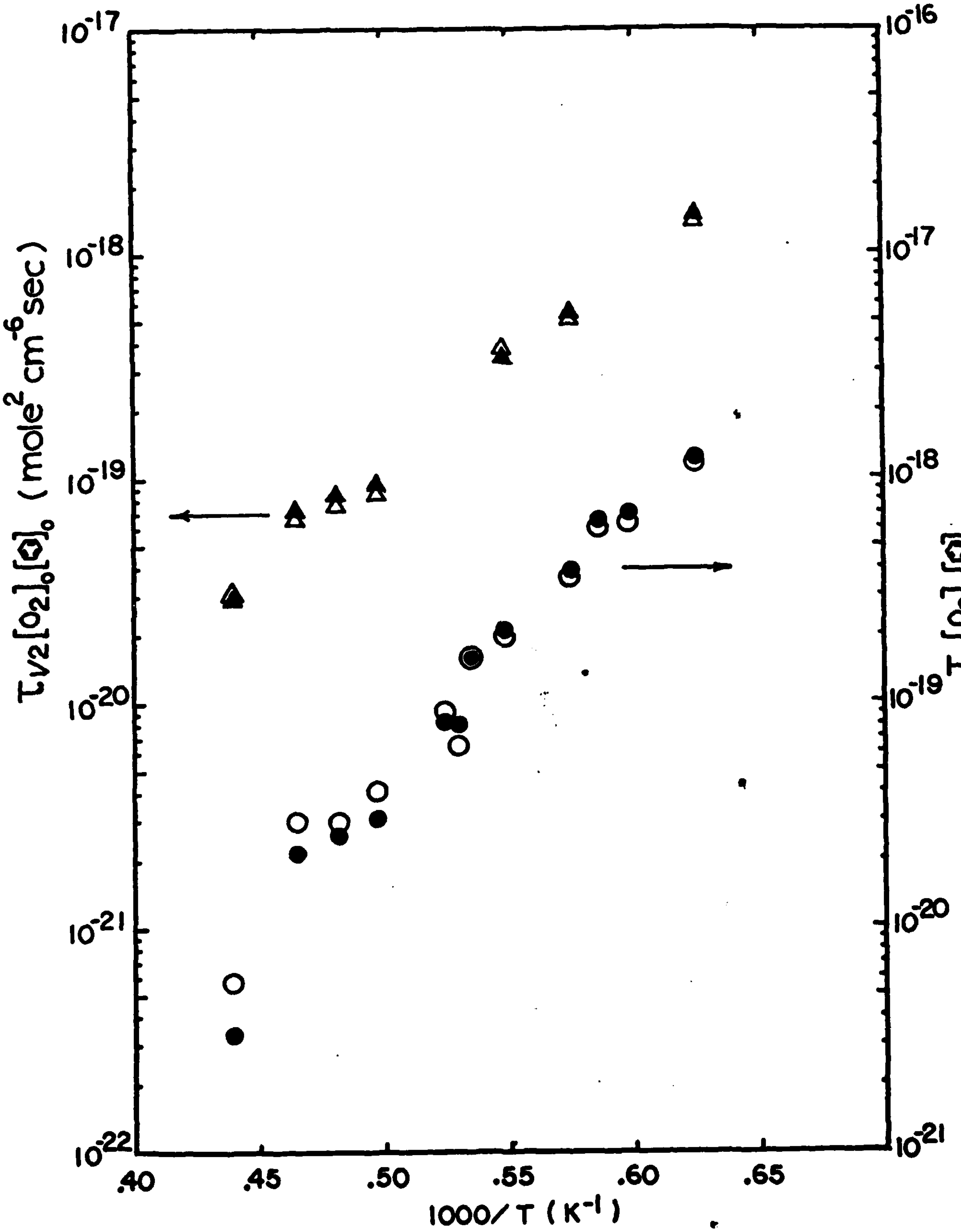

10^{-17}
10^{-18}
10^{-19}
10^{-20}
10^{-21}
10^{-22}
10^{-16}
10^{-17}
10^{-18}
10^{-19}
10^{-20}
10^{-21}
$\tau_{1/2}[O_2]_0[\text{⌬}]_0$ (mole^2 cm^{-6} sec)
$\tau_0[O_2]_0[\text{⌬}]_0$
.40
.45
.50
.55
.60
.65
1000/T (K^{-1})

Fig. 3.

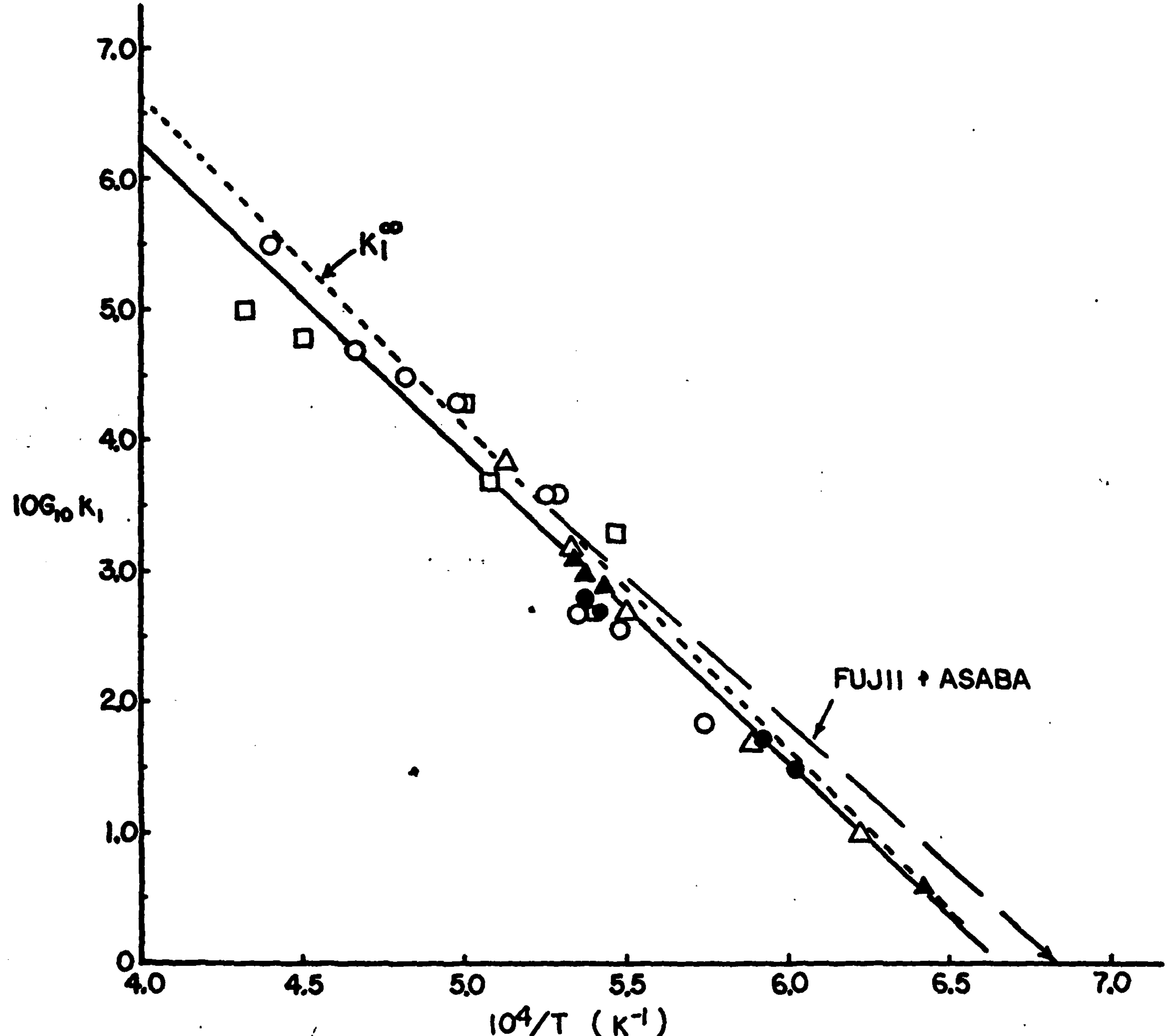

7.0
6.0
5.0
4.0
3.0
2.0
1.0
0
LOG10 K1
K1∞
FUJII + ASABA
4.0
4.5
5.0
5.5
6.0
6.5
7.0
10^4/T (K^-1)

Fig. 4.

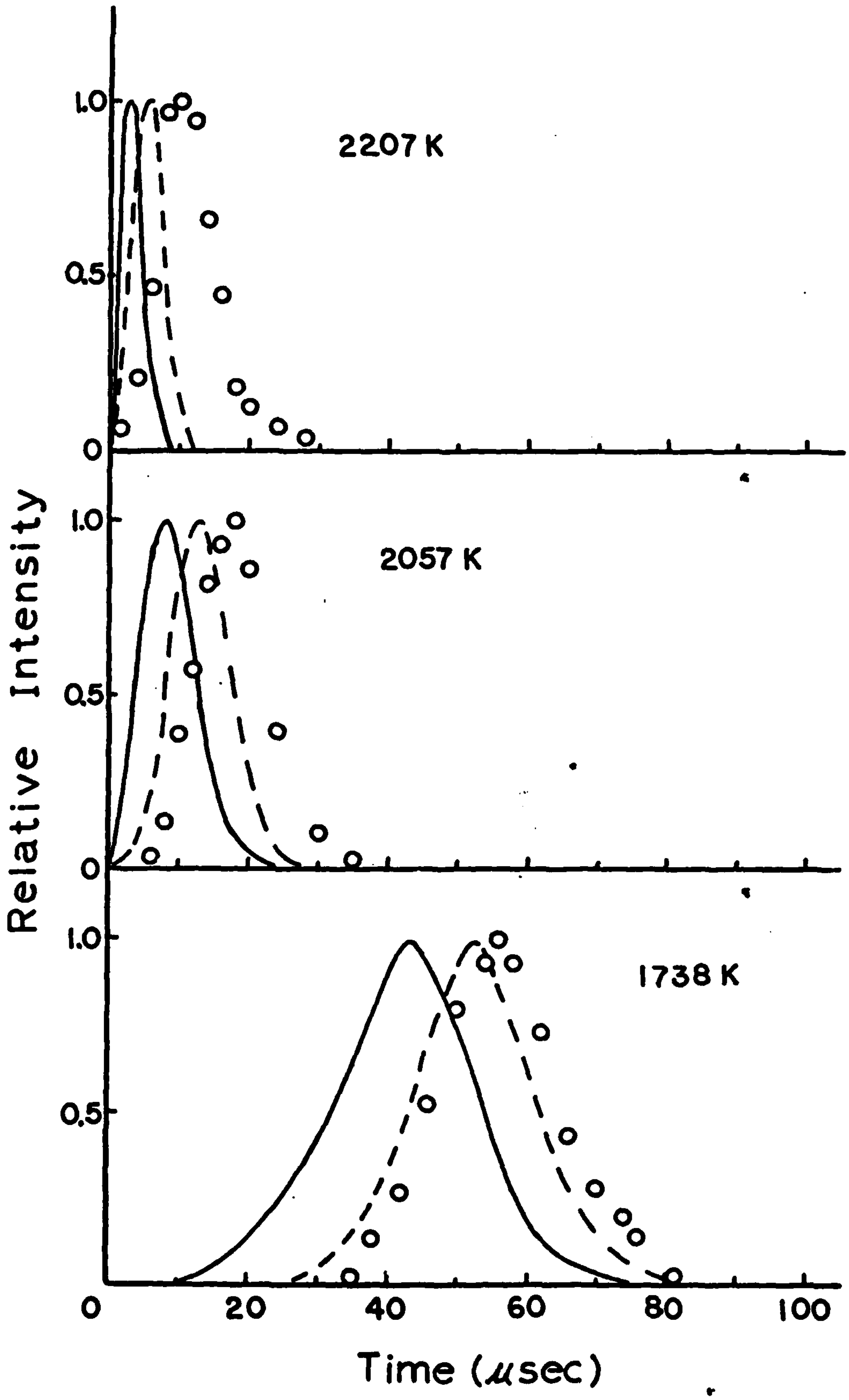
2207 K
2057 K
1738 K
Relative Intensity
Time (μsec)
0
0.5
1.0
0
20
40
60
80
100

Fig. 5.

END

FILMED

10-85

DTIC